

Network-based forecasting of climate phenomena

Article

Accepted Version

Ludescher, J., Martin, M. ORCID: <https://orcid.org/0000-0002-1443-0891>, Boers, N. ORCID: <https://orcid.org/0000-0002-1239-9034>, Bunde, A., Ciemer, C. ORCID: <https://orcid.org/0000-0002-4092-3761>, Fan, J. ORCID: <https://orcid.org/0000-0003-1954-4641>, Havlin, S. ORCID: <https://orcid.org/0000-0002-9974-5920>, Kretschmer, M. ORCID: <https://orcid.org/0000-0002-2756-9526>, Kurths, J., Runge, J., Stolbova, V. ORCID: <https://orcid.org/0000-0002-5574-3827>, Surovyatkina, E. ORCID: <https://orcid.org/0000-0001-5136-4988> and Schellnhuber, H. J. (2021) Network-based forecasting of climate phenomena. *Proceedings of the National Academy of Sciences of the United States of America*, 118 (47). e1922872118. ISSN 0027-8424 doi: <https://doi.org/10.1073/pnas.1922872118> Available at <https://centaur.reading.ac.uk/101629/>

It is advisable to refer to the publisher's version if you intend to cite from the work. See [Guidance on citing](#).

To link to this article DOI: <http://dx.doi.org/10.1073/pnas.1922872118>

Publisher: National Academy of Sciences

All outputs in CentAUR are protected by Intellectual Property Rights law, including copyright law. Copyright and IPR is retained by the creators or other copyright holders. Terms and conditions for use of this material are defined in the [End User Agreement](#).

www.reading.ac.uk/centaur

CentAUR

Central Archive at the University of Reading

Reading's research outputs online

Network-based Forecasting of Climate Phenomena

Josef Ludescher^{a,1,2}, Maria Martin^{a,1,2}, Niklas Boers^{a,b,c}, Armin Bunde^d, Catrin Ciemer^a, Jingfang Fan^{a,e}, Shlomo Havlin^f, Marlene Kretschmer^g, Jürgen Kurths^{a,h}, Jakob Rungeⁱ, Veronika Stolbova^j, Elena Surovyatkina^{a,k}, and Hans Joachim Schellnhuber^a

This manuscript was compiled on September 26, 2021

1 **Network theory, as emerging from complex-systems science, can provide critical predictive power for mitigating the global-warming crisis**
2 **and other societal challenges. Here we discuss the main differences of this approach to classical numerical modelling and highlight several**
3 **cases where the network approach substantially improved the prediction of high-impact phenomena: (i) El Niño events, (ii) droughts in the**
4 **Central Amazon, (iii) extreme rainfall in the Eastern Central Andes, (iv) the Indian summer monsoon, and (v) extreme stratospheric polar**
5 **vortex states that influence the occurrence of wintertime cold spells in northern Eurasia. In this Perspective, we argue that network-based**
6 **approaches can gainfully complement numerical modelling.**

climate-phenomena | forecasting | network theory | climate networks

1 If societies are able to anticipate disruptive events, they can take
2 measures to save thousands of lives and to avoid billions of eco-
3 nomic costs (1–5). A most evident, globally disruptive event is
4 certainly the current Covid-19 pandemia. Even though it seems im-
5 possible to accurately predict the emergence of such a virus itself,
6 the pandemia bears several characteristics that are also shared by
7 other disruptions: The general risk of something like this to happen
8 was known before, but economic and societal preparations to limit
9 harmful impacts are strongly dependent on a credible, science
10 based warning, preferably with significant time before the event
11 or at least before its full unfolding (the spreading in the case of a
12 virus) and with specifications of foreseeable impacts. Such a warn-
13 ing is not always possible, but there are promising new avenues.
14 Here, we describe our perspective on this research challenge from
15 the point of view of network theory and its usefulness for better
16 understanding and for forecasting specific climate phenomena.

17 Relevant climate phenomena that have the potential to pro-
18 duce major disruptions in societies are, for instance, the El Niño
19 phenomenon, the Indian summer monsoon and extreme weather
20 patterns like persistent heat waves, cold spells or rainstorms as
21 associated with stalling planetary Rossby waves (6). For instance,
22 a popular saying in India - that the “true finance minister” is the
23 monsoon - is based on the fact that water resources are vital
24 for India, where the rural economy accounts for about 45% of
25 GDP (7). El Niño occurrences are well known for their global im-
26 pacts on weather patterns and therefore societies. Floods and
27 heatwaves, especially concurring with droughts, directly affect hu-
28 mans and nature, and can wreak havoc in agriculture. Beyond
29 the climate system, highly challenging events of disruptive nature
30 are large-magnitude earthquakes, outbreaks of epidemics and,

on the individual level, physiological disasters like heart attacks.
These phenomena often emerge with little precursory signal or no
warning time at all, making effective adaptation challenging, if not
impossible. The pertinent lack of predictive power, however, is not
surprising, since most of those high-impact events are generated
by complex systems composed of many nonlinearly interacting
entities.

In the case of weather and climate, forecasting relies predom-
inantly on numerical models (8). Starting with Richardson in the
1920s (9), it has been a long way to the first successful prediction
(10) in 1950 and eventually to the highly sophisticated general
circulation and Earth system models of today (11). These simu-
lators rely on initial conditions (especially for weather forecasts,
i.e., the prediction of atmospheric dynamics for up to two weeks)
and boundary conditions (which are more relevant for seasonal
and longer-ranging forecasts, involving slower climate components
like the oceans) and deliver very good forecasts for a broad range
of physical quantities. However, their predictive power for certain
climate phenomena beyond the weather time-scale can be rather
limited: The dependence on precise initial and boundary conditions
and the necessity to simplify, inherent to any modelling approach,
as well as the chaotic nature of the system under study will hit hard
limits to further improvement (12, 13).

In spite of multiple efforts towards seamless prediction, a gap
remains in prediction skill between the sub-seasonal weather fore-
cast and the seasonal and longer climate predictions. Near-term
climate prediction is one of the Grand Challenges of the World
Climate Research Programme, WCRP (14). There have also been
other significant efforts in this domain, for instance, with the sub-
seasonal to seasonal (S2S) prediction project (15, 16). But in
many cases, numerical modelling still does, and also might con-

^aPotsdam Institute for Climate Impact Research, Potsdam, Germany; ^bFree University Berlin, Berlin, Germany; ^cUniversity of Exeter, Exeter, UK; ^dJustus-Liebig-Universität Gießen, Gießen, Germany; ^eSchool of Systems Science, Beijing Normal University, Beijing, China; ^fBar-Ilan University, Ramat-Gan, Israel; ^gUniversity of Reading, Reading, UK; ^hNizhny Novgorod State University, Nizhny Novgorod, Russia; ⁱGerman Aerospace Center (DLR), Institute of Data Science, Jena, Germany; ^jETH Zürich, Zürich, Switzerland; ^kSpace Research Institute of Russian Academy of Sciences, Moscow, Russia

Author contributions: J.L., M.M., N.B., A.B., C.C., J.F., S.H., M.K., J.R., V.S., E.S., and H.J.S. wrote the paper.

¹J.L. and M.M. contributed equally to this work

²To whom correspondence may be addressed. E-mail: josef.ludescher@pik-potsdam.de or maria.martin@pik-potsdam.de

The authors declare no competing interest.

62 tinue to leave vulnerable societies with insufficient warning time
63 ahead of climate phenomena, within as well as outside of the
64 above mentioned gap: There are types of climate phenomena that
65 still notoriously elude reliable long-term forecasting through numerical
66 modelling. For five specific climate phenomena examples
67 discussed below, network theory has led to (in some cases) considerably
68 earlier forecasts compared to state-of-the-art operational
69 forecasts, see (SI Appendix, Table S1).

70 Here we argue that the predictability limitations of existing operational
71 forecasts are partly due to the basic intention of numerical models: The
72 goal of faithfully mirroring the local nature of direct interactions in the
73 physical world. However, the models are not perfect mimics of nature.
74 Processes, e.g., turbulence, are not resolved at all or only at a possibly
75 insufficient resolution and tuned parametrisations have to be employed
76 (17). In particular, teleconnections present in observational data may
77 be not well represented or even absent within numerical models. Thus,
78 identifying and then analyzing the evolution of teleconnections with
79 time can provide an additional avenue to predicting large-scale climate
80 phenomena. The beginnings of this promising avenue can be traced back
81 to Sir Gilbert Walker into the early 20th century, when he first noticed
82 teleconnections (18) and has now gained a new and much broader
83 perspective through the advent of complex network analyses.

84 Here we suggest that the evolving interactions (manifesting, e.g.,
85 via correlations) between different and often rather distant locations
86 can provide new insights and serve as predictors for a large variety of
87 climate phenomena. The philosophy behind this approach is that even in
88 a simple system, composed for instance of two coupled nonlinear
89 oscillators, one will observe aleatoric behavior providing very limited
90 information when measuring the motion of each oscillator individually.
91 However, when evaluating the coupling between them, e.g., via
92 synchronization (as already detected in the 17th century by Christiaan
93 Huygens (19)) one will obtain new and valuable information about the
94 system (20). Analogously, while one might not necessarily extract
95 useful information from measurements of single locations on the globe,
96 the links, i.e., the interactions between the sites and their evolution
97 in time, can provide, as in the examples below, critical novel information
98 for forecasting.

101 Network Analysis Opens a Second Avenue

102 Consequently, we propose to complement the established state of the
103 art for predicting climate phenomena through explicit numerical modelling
104 by the maturing approach of network theory (21–23). The idea is to
105 obtain additional information about the climate system by capturing the
106 connectivity of different locations (including long-distance ones),
107 through measuring the similarity in the evolution of their physical
108 quantities. This similarity between different locations (nodes) can be
109 quantified by different linear and non-linear measures like Pearson
110 correlation, event synchronization, mutual information, transfer entropy,
111 partial correlations or Granger causality. For an overview of the
112 different methods, see (24, 25).

113 The similarity is then translated into links connecting the nodes in
114 the network and measuring cooperativity, i.e., the property of not
115 acting independently of each other. Commonly, cutoff thresholds are
116 applied on these similarity measures to select only the statistically
117 significant links. These thresholds can be obtained by analyzing
118 surrogate data, e.g., shuffled versions of the original time series
119 or synthetic time series that match the relevant statistical properties
120 of the original time series. For more details on surrogate

121 methods, see (24, 25). For an illustration of a network framework,
122 see Fig. 1.

123 The final network can be represented by an adjacency (connectivity)
matrix A , which encodes the links between the nodes or their absence
and is defined as

$$A_{ij} = \begin{cases} \text{non-zero, if there is a link from node } j \text{ to node } i \\ 0, \text{ otherwise} \end{cases}$$

124 The value of the element A_{ij} represents the weight of the link.
125 Links connecting nodes to themselves are not included, i.e.,
126 $A_{ii} = 0$. If the links are not directed, then the adjacency matrix
127 is symmetric, $A_{ij} = A_{ji}$. However, links can also be defined as
128 directed links, with a starting node j and a target node i . For
129 instance, in the case of correlation-based links, a direction can be
130 defined via the sign of the time lag of the cross-correlation function.
131 When links are directed, A is generally non-symmetric $A_{ij} \neq A_{ji}$.

132 The so obtained adjacency matrix allows to calculate network
133 quantities like in- and out-degrees, clustering coefficients or
134 betweenness coefficients of nodes. For a detailed description of these
135 and other network quantities, see (21, 22). Many of these quantities,
136 which represent topological features of the network, have a physical
137 interpretation. For example, it was found by analysing advection-
138 diffusion dynamics on model background flows that a high absolute
139 flow velocity coincides with a high node degree, i.e., a high number
140 of links attached to a node (26).

141 While teleconnections can be emerging properties in dynamical
142 models, which mainly concentrate on data at specific grid cells and
143 their immediate neighbours, the basis of the network approach is
144 the direct analysis of the links between grid points of a large variety
145 of distances and their temporal evolution. This approach avoids the
146 necessity to mimic the entire climate system, enabling the forecasters
147 instead to pursue specific questions about particular non-local
148 phenomena. Since network-based prediction schemes often rely only
149 on assessing the current state of the regarded system, measurement
150 errors play a much smaller role for them than for numerical models,
151 where small errors in the initial conditions can lead to exponentially
152 increasing errors in the prediction, as it can be the case for weather
153 forecasting (8, 27).

154 In contrast to, e.g., online social networks, where the existence
155 of the structure is already known and subject to direct analysis, the
156 existence and structure of networks in the climate context is often
157 not obvious – they can be purely functional. In this respect, climate
158 networks are comparable to networks in neuroscience, where the
159 structural networks of synapses can be different from the functional
160 network derived from the connectivity of time series, e.g., EEG
161 measurements (28).

162 In the following, we focus on forecasting and highlight several
163 cases where the climate-network (24, 29–31) approach substantially
164 improved the prediction of high-impact climate phenomena: 1) El Niño
165 events (32–38), 2) droughts in the Central Amazon (39), 3) extreme
166 rainfall in the Eastern Central Andes (40, 41), 4) the Indian summer
167 monsoon (42–44), and 5) extreme stratospheric polar vortex states
168 (45, 46).

169 For most of these climate network-based analyses, the initial
170 motivation was to better understand and describe the regarded
171 climate phenomena and not primarily the discovery of a new
172 forecasting method, which often happens serendipitously. Generally,
173 there is currently no recipe to follow to surely obtain a network-
174 based prediction algorithm for a specific climate phenomenon or
175 to rule out that a network approach can address the phenomenon.
176 However, complex networks provide ideal tools for data exploration

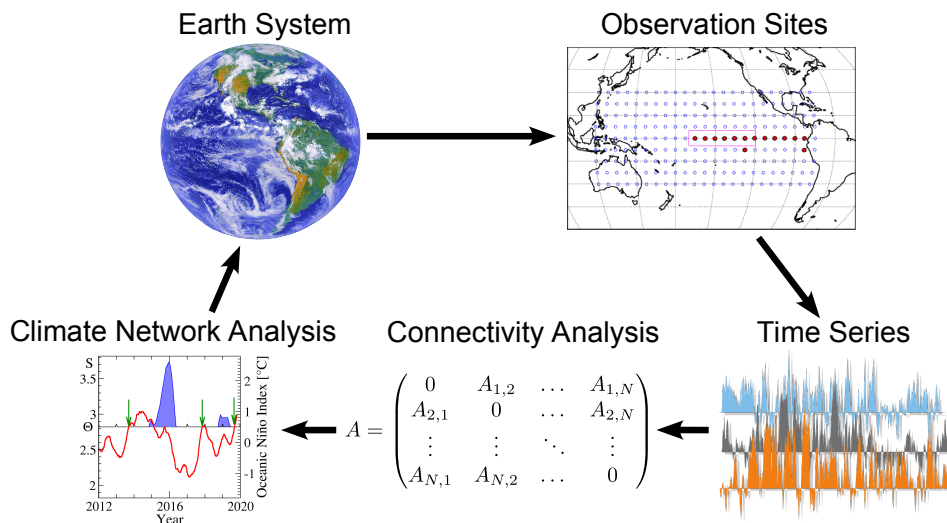


Fig. 1. The climate-network framework as a tool for prediction. Observational data of physical quantities, e.g., temperatures, are available at different geographical locations. These data can be used directly or via a reanalysis (numerical weather model) which assimilates and maps them onto a regular grid. Thus, for each node (observational site or reanalysis grid point) of the climate network, a time series of the regarded physical quantity is available. Cooperativity between nodes can be detected from the similarity in the evolution of these time series and translated into links connecting the corresponding nodes. The links or their strengths may change with time. These nodes and their links constitute the evolving climate network, which can be represented by the adjacency (connectivity) matrix A . The analysis of this network can enable early predictions of climate phenomena and provide insights into the physical processes of the Earth system. For example, for forecasting El Niño, the nodes are in the Pacific and the links are between the El Niño basin (full red circles) and the rest of the tropical Pacific (open blue circles). The rising of the network's mean link strength S (red curve) above a certain threshold Θ serves as a precursor (green arrows) for the start of an El Niño event (blue areas) in the subsequent calendar year (32). Parts of the figure are from: NASA, adapted from (32), created by Norbert Marwan.

177 to uncover spatial and temporal patterns in the data that can later
 178 potentially be explained with domain knowledge about the phe-
 179 nomenon leading to new physical insights. When this is the case,
 180 as for some of our examples below, then the discovered relation-
 181 ships may enable the development of new forecasting methods,
 182 which at this point could be entirely detached from the original
 183 climate network-based analyses that led to their discovery. How-
 184 ever, network-based quantities can potentially also serve as direct
 185 predictors in a forecasting algorithm if the underlying processes
 186 are not yet identified, as is the case in our first example.

187 El Niño

188 El Niño-events (49–51) are part of the El Niño-Southern Oscillation
 189 (ENSO), the most important driver of interannual global climate
 190 variability. ENSO can be perceived as a self-organized dynamical
 191 see-saw pattern in the tropical Pacific Ocean-atmosphere system,
 192 featured by rather irregular warm (“El Niño”) and cold (“La Niña”)
 193 excursions from the long-term mean state.

194 The existing operational El Niño predictions have been espe-
 195 cially limited by the so-called spring barrier, obscuring the
 196 anomaly's onset until about six months before its beginning (51, 52).
 197 In contrast, the climate network-based prediction method can cross
 198 this barrier and roughly double the pre-warning time to about 1y
 199 ahead (32). For example, in September 2013, the method fore-
 200 casted the onset of an El Niño event in 2014 with 75% probability
 201 and based on this, a warning was issued (33). The forecast turned
 202 out to be correct as an extreme El Niño event has started in 2014
 203 (53) and ended in 2016. For comparison, in December 2013, i.e.,
 204 3 months after the network-based forecast, the most far-reaching
 205 plume-based forecast of the International Research Institute for
 206 Climate and Society/Climate Prediction Center (IRI/CPC) predicted
 207 a neutral event with 46% probability, an El Niño with 44%, and a
 208 La Niña with 10% for August-September-October 2014 (54).

209 This successful prediction was based on a detailed analysis of
 210 the meteorological connectivity of locations inside the so-called El
 211 Niño-basin with locations distributed across the rest of the Pacific
 212 (32). This analysis area was chosen since the evolution of the
 213 ENSO takes place across the Pacific. Previous studies (30, 55)
 214 had found that the connectivity usually drops strongly during an El
 215 Niño event. Accordingly, the cooperativity has to increase before an
 216 event, and this feature serves as the basis for the early prediction.

217 To obtain a measure for the cooperativity, the approach builds
 218 on daily surface atmospheric temperatures at grid points (“nodes”)
 219 in the tropical Pacific (see map in Fig. 1), obtained from a reanal-
 220 ysis (56). The time evolution of the links between the temperature
 221 nodes inside the “El Niño basin” (14 nodes) and the nodes out-
 222 side the basin (193 nodes) is analyzed. The strengths of these
 223 2702 links are derived from the magnitudes of the lagged cross-
 224 correlation functions between the temperature time series at the
 225 corresponding sites. For further details, see the original publica-
 226 tions (32, 33). The rising of the network's mean link strength S
 227 above a certain threshold Θ serves as a precursor for the start of
 228 an El Niño event in the subsequent calendar year. This empirical
 229 threshold was optimized using a learning phase (1950-1980) and
 230 the approach's skill was tested in a hindcasting phase (1981-2011),
 231 see Fig. 2A, B. Figure 2C compares the prediction accuracy of the
 232 network approach via a receiver operating characteristic (ROC)-
 233 analysis with the 6- and 12-month forecasts based on dynamical
 234 climate models (57, 58). Based on this analysis, the network ap-
 235 proach considerably outperforms conventional 6-month and 1-year
 236 forecasts through dynamical modelling. The method was tested
 237 and validated, e.g., by discarding 80% of the nodes outside the
 238 El Niño basin randomly, leading to about the same prediction per-
 239 formance and by randomly (block) shuffling the data to obtain
 240 statistical error estimates for the observed performance of the
 241 method (32).

242 The network approach has proven its operational skill not

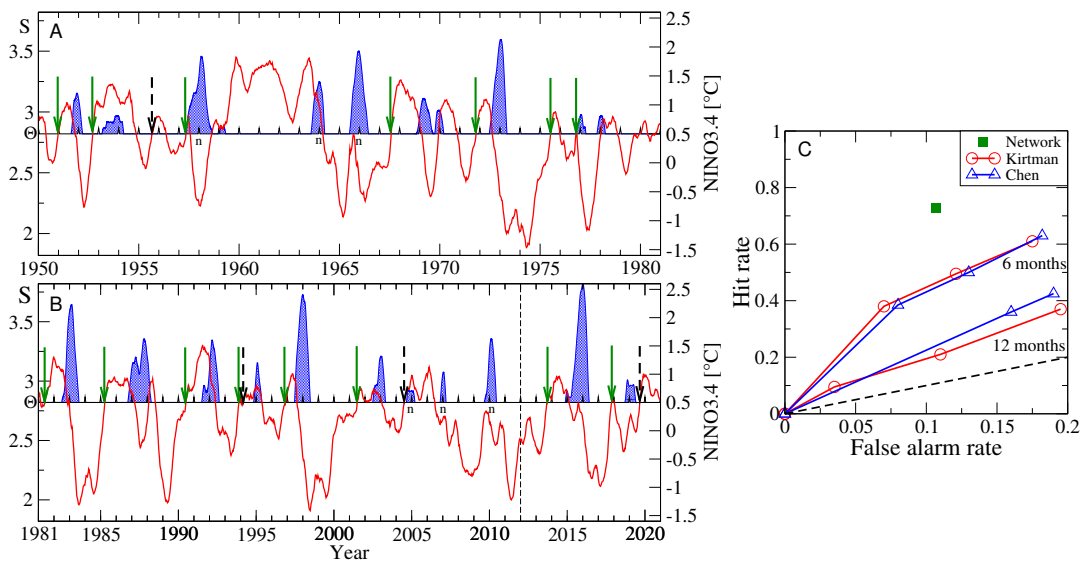


Fig. 2. The El Niño forecasting algorithm, updated figures from the original publication (32). (A, B) The mean link strength $S(t)$ (red curve) of the climate network (see Fig. 1) is compared to a decision threshold Θ (horizontal line, here $\Theta = 2.82$) (left scale) with the Oceanic Niño Index (ONI) (right scale). The ONI is defined as the 3-month running mean of the sea surface temperature anomalies in the Niño3.4 area in the Pacific (pink rectangle in Fig. 1). When the link strength crosses the threshold from below outside of an El Niño episode, an alarm is given and the start of an El Niño in the following calendar year is predicted. El Niño episodes (when the ONI is above 0.5°C for at least 5 months) are shown by blue areas. (A) shows the learning phase 1950-1980, where the decision threshold was optimized. In (B), the threshold obtained in (A) is used to hindcast and forecast El Niño episodes. The hindcasting and forecasting phases are separated by a dashed vertical line. Correct predictions are marked by green arrows, false alarms by dashed arrows. The index n marks unpredicted El Niño episodes. The lead time between a correct alarm and the beginning of the El Niño episodes is 1.01 ± 0.28 y, while the lead time to the maximal Niño3.4 value is 1.35 ± 0.47 y (32). (C) The prediction accuracy [Receiver Operating Characteristic (ROC)-type analysis]. In a ROC analysis, the hit rate (the number of correctly predicted events divided by the total number of events) is plotted against the false alarm rate (the number of false alarms divided by the number of non-events). The figure compares the performance of the network-based method (forecasting and hindcasting phase, 1981-2020, see (B)) with the 6- and 12-mo forecasts based on climate models (57, 58). In contrast to ensemble methods, the network-based “ROC-curve” is a single point since, by construction, the method does not allow to arbitrarily increase the hit rate at the expense of increasing the false alarm rate. The black dashed line shows the diagonal corresponding to random predictions.

merely in hindcasting but also in forecasting since it was introduced in 2012: Between 1981 and 2020, i.e., after the learning phase, the El Niño-onset predictions are correct to 73%, and the no-show predictions are correct even to 89%, see Fig. 2. Based on random guessing with the climatological average El Niño occurrence probability, the corresponding p-value is $5.8 \cdot 10^{-5}$ and for the forecasting phase alone $p = 0.029$ (8 out of 9 forecasts were correct).

The question of which physical processes generate the cooperative mode and how they are related to the El Niño-buildup is still open and offers interesting new research opportunities. Possible answers lie in an understanding of the Walker circulation as a synergetic phenomenon, of slow oceanic Rossby waves or of oceanic turbulence structures. The relationship between the cooperative mode and the El Niño-buildup should be also present in dynamical models, which makes this relationship a useful test criterion for a model’s ability to accurately reflect the underlying mechanisms.

Climate network derived quantities have also shown predictive skill for El Niño/ENSO in other studies (34–38, 59) and show that an upcoming El Niño provides early warning signals, which can be picked up by suitable climate networks.

Predicting Droughts in the Central Amazon

Droughts have severe impacts on ecosystems all around the globe. They increase tree mortality and the risk of wildfires, which threaten forests in addition to ongoing large-scale deforestation. The Amazon rainforest has experienced several extreme droughts in the last decades, during which the rainforest temporarily turned from a carbon sink to a carbon source (60). More persistent and more

frequent droughts in the Amazon increase the risk of a large-scale transition from rainforest to savanna (61). A dieback of the rainforest would shift this ecosystem from a carbon sink into a carbon source (62).

Although the tropical Atlantic Ocean is the main source of moisture inflow into South America (63), it has long been thought that droughts in the Amazon basin are dominantly caused by El Niño events and associated longitudinal displacements of the atmospheric Walker circulation. Only more recently, it has been suggested that sea surface temperature (SST) anomalies in the tropical Atlantic Ocean could provoke hydrological extremes in the Amazon as well (64).

Based on this hypothesis, a complex network was applied to identify oceanic regions with a strong impact on Amazon rainfall. By introducing a bi-variate network approach (39), it was possible to reveal the two regions in the tropical Atlantic ocean where SST anomalies have the strongest impact on seasonal-scale rainfall anomalies in the central Amazon (Fig. 3a,b). The spatial pattern revealed with this network-based data analysis is then explained in terms of the relevant atmospheric and oceanic processes. It was shown in (39) that the development of an SST dipole between these regions in the northern and southern tropical Atlantic and associated latitudinal shifts of the Intertropical Convergence Zone lead to large-scale droughts in the central Amazon.

The analysis of the correlation structure between SST anomalies in the two identified tropical Atlantic regions reveals clear early-warning signals for droughts in the Amazon (Fig. 3c). A drought warning is issued once the correlation turns significantly negative, indicating the beginning of the development of the tropical Atlantic SST dipole. Based on this scheme, six out of the seven most se-

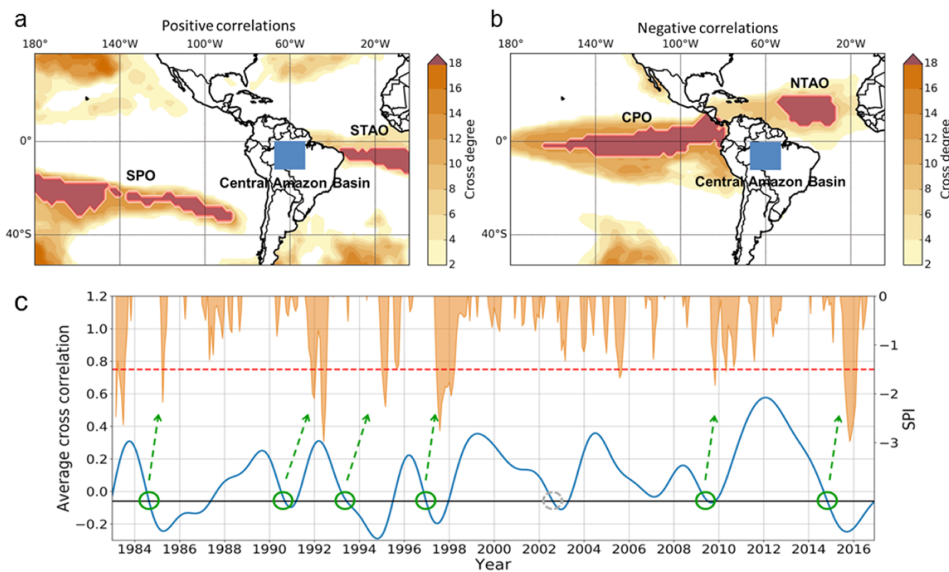


Fig. 3. Drought prediction analysis based on correlation structure of SST anomalies in the northern and southern tropical Atlantic Ocean. a,b) Cross degree between SSTs and continental rainfall anomalies. For each SST grid cell of the Atlantic and Pacific Ocean, the cross degree towards rainfall in the Central Amazon Basin (blue box) is shown, for a) positive and b) negative correlations. Darker shading indicates a larger cross degree, implying a larger number of links, and thus significant correlations with rainfall at more grid points in the Central Amazon Basin. Red areas outline coherent oceanic regions with the 20% highest cross degrees. c) Early-warning signal for droughts in the Central Amazon Basin. The time evolution of the average cross correlation of the Northern and Southern Tropical Atlantic Ocean (blue) is compared with the standardized precipitation index (SPI, orange) of the Central Amazon Basin. Negative SPI anomalies with SPI < -1.5 (red dotted line) indicate severely dry periods. A drought event is predicted within the following one and a half years whenever the average cross correlation between the SST anomalies falls below an empirically found threshold of -0.06. Green circles indicate a matching prediction, with one false alarm in 2002 indicated by a grey circle, where the threshold is crossed but no drought took place in the direct aftermath. The temporal evolution of the average cross correlation shown here is smoothed using a Chebyshev type-I low-pass filter and cutoff at 24 months. Figures from (39) (CC BY).

301 vere droughts in the central Amazon that occurred during the last
 302 four decades were successfully hindcasted at lead times between
 303 12 and 18 months.

304 Extreme Rainfall in the Eastern Central Andes

305 During the core season of the South American monsoon from
 306 December through February, the eastern slopes of the Central
 307 Andes are frequently affected by extreme rainfall events. These
 308 events can lead to floods and landslides with devastating socioeco-
 309 nomic impacts, but until the development of the network approach
 310 (40, 41), no early-warning scheme had been proposed.

311 Complex networks were again used as a data-exploration
 312 method to reveal patterns that might be useful for prediction when
 313 combined with mechanistic insights. The spatiotemporal structure
 314 of those extreme rainfall events (above the 99% percentile), as
 315 inferred from high-resolution satellite data, can be mapped onto
 316 a directed and weighted network: The link weights between two
 317 grid points are a measure for how often two grid points show a
 318 time-delayed, significantly similar precipitation event pattern, and
 319 the direction is determined by the temporal sequence of the events.
 320 The resulting network allows for identifying the source and the
 321 sink regions of extreme precipitation across the South American
 322 continent. SI Appendix Fig. S1 shows that the Intertropical Con-
 323 vergence Zone and the northern Amazon are a source of extreme
 324 events, while the central parts of South America are sink regions
 325 of extremes.

326 Surprisingly, the network approach reveals that the exit region of
 327 the low-level monsoonal wind flow in southeastern South America
 328 turns out to be a source area of extreme rainfall events. The di-
 329 rected network structure allows to infer that events occurring there

330 tend to be followed by further events along a narrow band extend-
 331 ing northwestward to the Bolivian Central Andes, and thus in the
 332 opposite direction of the low-level monsoon circulation. Combining
 333 the results of this data exploration with process knowledge reveals
 334 the mechanisms underlying these extreme events and opens the
 335 door for prediction. A detailed analysis of the atmospheric condi-
 336 tions exhibits that not the rainfall systems themselves, but rather
 337 the atmospheric conditions that favor the development of large
 338 convective systems and thus lead to extreme rainfall, propagate
 339 against the direction of the monsoon circulation (41). These atmo-
 340 spheric conditions are determined by westward moving Rossby
 341 wave trains that originate from the southern Pacific Ocean and turn
 342 northward after crossing the southern tip of the continent. The
 343 interaction of the pressure anomalies embedded on these Rossby
 344 wave trains with the warm, moist monsoon flow from the tropics
 345 leads to the propagation of extreme rainfall from southeastern
 346 South America northwestward to the Central Andes.

347 The so-gained knowledge establishes a forecasting rule for
 348 extreme rainfall in the eastern Central Andes based on two precon-
 349 ditions, namely (i) strong rainfall in southeastern South America,
 350 and (ii) an anomalously deep low-pressure system over northwest-
 351 ern Argentina. With a lead time of two days, this forecast rule
 352 correctly predicts 60% (and 90% during El Niño conditions) of the
 353 extreme rainfall events in the eastern Central Andes (41). Note
 354 that these 60% true positives correspond to a Heidke Skill Score
 355 of 0.47 and thus clearly outperform a random forecast, for which
 356 this score would yield a value of zero. The better prediction skill
 357 during El Niño conditions can be explained by the fact that the
 358 atmospheric pattern described above, based on which the forecast
 359 rule has been established, occurs more often, and more concisely,
 360 during these episodes.

361 Teleconnections for extreme rainfall do not only operate at regional to continental, but also at global scales (65). In particular, 362 atmospheric Rossby waves can be identified as dominant transcontinental processes. The forecasting potential of continental and 363 global synchronization patterns for extreme rainfall has so far only 364 been systematically assessed in a few cases and should be exploited for other regions. Moreover, extreme-rainfall teleconnection 365 patterns determined from observational data can, in principle, yield 366 a methodological framework to benchmark and constrain atmospheric general circulation models with respect to their capability 367 to reproduce these patterns. 368 369 370 371

372 Indian Summer Monsoon

373 The Indian summer monsoon is an intense rainy season lasting 374 from June to October. The monsoon delivers more than 70% 375 of the country's annual rainfall, which is the primary source of 376 freshwater for India. Although the rainy season happens every 377 year, the monsoon onset and withdrawal dates vary within a month 378 from year to year. Such variability greatly affects life and property 379 of more than a billion people in India, especially those living in 380 rural areas and working in the agricultural sector, which employs 381 70% of the entire population. Only Kerala in South India receives 382 an official monsoon forecast (47) two weeks in advance, while 383 the other 28 states rely on the operational weather forecast of 384 about 5 days (47). The demand for an earlier monsoon forecast is 385 highest in central India, which is most exposed and vulnerable to 386 droughts before the monsoon onset. Moreover, while under climate 387 change, severe storms and floods during the monsoon withdrawal 388 are becoming more frequent, there is currently no official forecast 389 for the withdrawal date.

390 Exploratory network-based analyses of extreme rainfall across 391 the Indian subcontinent (42, 43) enabled the identification of geographical domains displaying far-reaching links, influencing distant 392 grid points. Especially North Pakistan and the Eastern Ghats 393 turn out to be crucial for the transport of precipitation across the 394 subcontinent (43). 395

396 The combination of the network-based analysis and nonlinear 397 dynamics in the tipping-elements approach (44) allowed to uncover 398 the critical nature of the spatiotemporal transition to the monsoon. 399 It was found that the temporal evolution of the daily mean air 400 temperature and relative humidity exhibit critical thresholds on the 401 eve and at the end of the monsoon. The spatial analysis of the 402 critical growth of the fluctuations (66) in the weekly mean values 403 of the same variables revealed the same two geographical areas 404 with maximum fluctuations (Fig. 4a-c): the Eastern Ghats (EG) 405 and North Pakistan (NP). A highly developed instability occurring 406 in these regions creates the conditions necessary for the spatially 407 organized and temporally sustained monsoon rainfall. Thus, the 408 two critical regions appear to play the role of the tipping elements 409 of the monsoon system. The most interesting feature is how the 410 tipping elements are connected: on the eve of the onset and 411 the withdrawal of the monsoon in the central part of India, the 412 temperature and relative humidity in two tipping elements equalize 413 (Fig. 4d). This insight creates the foundation for predictions of the 414 monsoon timing.

415 Based on this knowledge, a scheme was developed for forecasting 416 the upcoming monsoon onset and withdrawal dates in the 417 central part of India 40 and 70 days in advance, respectively, thus - 418 considerably improving the time horizon of conventional forecasts 419 (44). The new scheme has proven its skill (73% of onset and 84% 420 of withdrawal predictions correct) not only in retrospective (for the

421 years 1951-2015) but showed to be successful in the prediction of 422 future monsoons already five years in a row since its introduction 423 in 2016 (68). The methodology appears to be robust under climate 424 change and has proven its skill also under the extreme conditions 425 of 2016, 2018 and 2019.

426 The approach creates new monsoon-forecasting possibilities 427 around the globe, for instance, for the African, Asian and American 428 monsoon systems. In particular, it also offers the possibility for 429 regional monsoon forecasting schemes, like the above one for the 430 central part of India.

431 Stratospheric Polar Vortex

432 The Northern Hemisphere extratropical stratosphere in boreal winter 433 is characterized by a westerly circumpolar flow, the stratospheric 434 polar vortex (SPV) (69). The strength of the SPV can influence the 435 tropospheric mid-latitude circulation and a weak SPV increases 436 the chances of cold air outbreaks there. Thus, extremely weak 437 SPV states can lead to cold spells in parts of North America and 438 Eurasia. Given the rather persistent surface impacts, the SPV 439 is also an important source of subseasonal to seasonal (S2S) 440 predictability for winter weather (70). To predict extremely weak 441 and strong SPV states, a climate network was constructed via 442 the Peter Clark Momentary Conditional Independence (PCMCI) 443 algorithm (45, 71) and has been successfully applied to identify 444 the precursor processes of these states.

445 While in the previous climate network examples, nodes were 446 single grid points on the globe, in this approach, each node of the 447 network stands for an individual sub-process and the links, derived, 448 for instance, from partial correlations, have a causal interpretation 449 (45, 46, 71, 72). A quantitative representation of a sub-process 450 (node) might be, for instance, the mean value of a physical quantity 451 over a particular spatial area (e.g., sea level pressure anomalies 452 over the Ural Mountains region).

453 Then the aim is to estimate a directed network representation 454 of the regarded system's sub-processes, i.e., to identify which 455 sub-processes causally influence which other sub-processes (for 456 details, see (71)). This goal is addressed by discriminating between 457 the direct causal connections between the sub-processes and 458 spurious, non-causal correlations (71, 72). The latter can arise due 459 to common causes of two regarded sub-processes, intermediate 460 mediating processes or autocorrelations in the sub-processes. 461 The PCMCI algorithm identifies those spurious correlations and 462 removes them from the network.

463 At the start of the SPV analysis, potential relevant variables 464 affecting vortex variability were expected in variables such as sea 465 surface temperatures, sea level pressure and lower stratospheric 466 poleward eddy heat flux. From these fields, regional precursors 467 indices were first formed by cross-correlating the fields against the 468 polar vortex time-series and then averaging over the significantly 469 correlated regions. In the next step, these precursors indices 470 were then evaluated using the PCMCI algorithm for their causal 471 interactions. Thus, while domain knowledge was crucial to choose 472 the input variables, selecting the exact precursor regions as well as 473 identifying and quantifying the involved causal processes was done 474 using the algorithm described in (46, 72), which yields statistically 475 more reliable estimates than relying on Granger Causality (71).

476 The algorithm enabled the prediction of stratospheric polar 477 vortex behavior with predictive skill up to 45 days for extreme 478 15-day-mean events (46). For instance, the scheme hindcasts 479 58% of the extremely weak polar-vortex states with a lead time 480 of 1-15 days and a false alarm rate of only about 5%. Dynamical

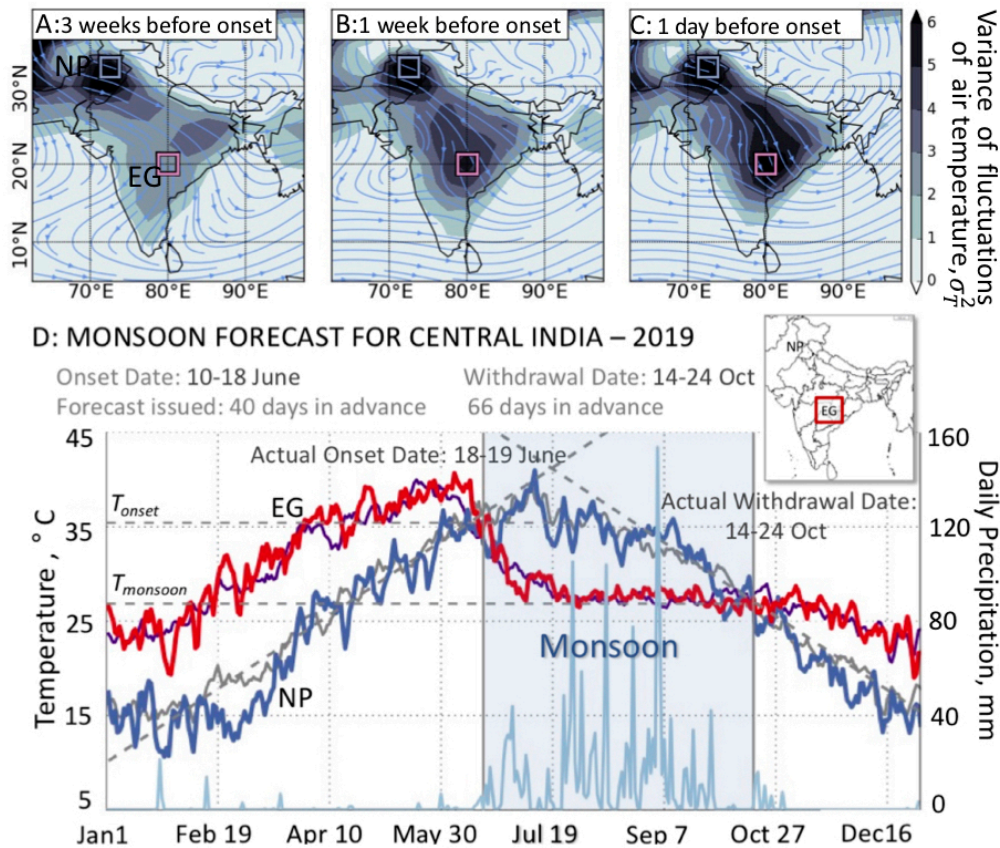


Fig. 4. Tipping elements of the Indian summer monsoon (ISM): forecast of onset and withdrawal dates for 2019 (based on the methodology in (44)). The Tipping elements of the ISM are geographical regions in North Pakistan (NP) and the Eastern Ghats (EG), which are revealed by the pre-monsoon growth of the variance σ_T^2 of fluctuations of the weekly mean values of the near-surface air temperature T , (A) 21 days, (B) 7 days, and (C) 1 day before the monsoon onset in the EG. Two boxes, where σ_T^2 is maximal, show the location of the tipping elements. The composites of σ_T^2 and the 700 hPa winds (indicated by the blue lines) for the period 1958–2001 from the ERA40 reanalysis data set (73) are shown in A-C. (D) Forecasting scheme of the onset and withdrawal dates for central India in the EG-region for 2019 based on daily mean near-surface (1000 hPa) air temperatures (NCEP/NCAR) (56, 74) in 2019 in the EG (red) and NP (blue), and the previous 5-years average temperature in the EG (purple) and NP (gray). Vertical grey lines represent the forecasted monsoon onset and withdrawal dates, which we call the tipping points of the monsoon. The tipping points occur when the temperatures in the EG and NP (the tipping elements of the monsoon) become equal, which happens twice during a year. At the end of May, the temperature in the EG decreases from its maximum value; then, it reaches a critical threshold (T_{onset}), and an abrupt transition occurs - the temperature inevitably falls, and the rainy season begins in the EG region. At the same time, the temperature in NP increases, and the two time-series intersect at T_{onset} at the onset date of the monsoon in the EG. In October, when the temperature in NP falls below at the second intersection of the two time-series, the monsoon withdraws from the EG. This feature allows to estimate the dates when the two critical temperatures (T_{onset} and $T_{monsoon}$) are reached and to forecast the onset and withdrawal dates of the monsoon. (See details in (44)). The daily precipitation in the EG region obtained from NOAA (67) is shown superimposed in light blue. The sudden increase and decrease in precipitation coincide with the monsoon period defined by the light blue band. The results of forecasts for the period 2016–2020 are presented in (68). Parts of the figure are from (44), reprinted with permission from John Wiley and Sons, copyright American Geophysical Union.

481 forecast methods can provide predictability up to 30 days for daily
 482 events, so-called sudden stratospheric warmings, but the prediction
 483 lead time varies strongly for individual events and is usually much
 484 shorter (48).

485 This approach of reconstructing causal interactions is a power-
 486 ful tool in Earth system sciences (72): It can be applied to test
 487 specific hypotheses about interaction mechanisms or to weigh
 488 the importance of components as gateways for spreading per-
 489 turbations in the network. But it also offers a novel approach to
 490 prediction: For prediction targets as different as the amount of
 491 Indian summer monsoon rainfall (75) and seasonal Atlantic hur-
 492 ricane activity (76), precursors with lead times of several months
 493 could be identified. Additionally, the algorithm also allows more
 494 process-based model evaluations (77) beyond simple correlation
 495 analyses to understand potential biases in representing telecon-
 496 nection pathways. This might, in particular, be useful in the form
 497 of hybrid forecasts (78) which combine numerical models with

statistical methods.

498
 499 The PCMCI algorithm is particularly useful if the main goal is
 500 understanding the underlying mechanisms of different processes
 501 by reconstructing causal relationships hidden in correlations of
 502 observed data. The algorithm requires sufficient domain expertise
 503 to optimally pre-select the variables and processes of the phenom-
 504 ena one is interested in and can be sensitive to different parameter
 505 settings. Although causal discovery algorithms have been success-
 506 fully applied to high-dimensional settings as well (including the here
 507 discussed SPV case, see also (71, 79)), a low-dimensional, parsimonious
 508 set of variables representing the considered mechanisms is often
 509 beneficial to reduce the number of statistical independence
 510 tests in order to assure interpretability of results. In contrast, com-
 511 plex correlation networks provide a more explorative approach,
 512 helping to detect patterns in large high-dimensional data, which
 513 can give rise to new hypotheses, which could, in turn, be tested
 514 with the PCMCI approach.

515 Climate Networks and Artificial Neural Networks

516 Extending the avenues for climate-phenomena forecasting beyond
517 numerical modelling is not limited to climate network theory. Arti-
518 ficial neural networks (ANNs), and especially their currently most
519 popular application, deep learning (80, 81), are inspired by the
520 functioning of the brain and are also composed of nodes ("neu-
521 rons"), which are connected (linked) to other nodes. However,
522 the similarity to climate networks is primarily structural: In climate
523 networks the individual nodes represent grid locations or physi-
524 cal processes, thereby creating an alternative description of the
525 physical world. By contrast, the nodes in ANNs and their links
526 (the ANN's architecture) have generally no physical meaning and
527 the link (and bias) weights, trained on the data, create an internal
528 representation of useful aspects of the physical world. If enough
529 training data have been presented to a suitable ANN, it is able to
530 capture characteristics of the underlying system and make pre-
531 dictions. For instance, deep learning has been recently proposed
532 to forecast the El Niño-Southern Oscillation (82) and the amount
533 of Indian summer monsoon rainfall (83). Furthermore, ANNs and
534 other machine-learning techniques have been successfully applied
535 to a wide range of weather and climate questions and can be
536 powerful tools for tackling climate change; see (84) for a detailed
537 review. However, an issue at the forefront of research remains the
538 black-box character of ANNs (85), although promising advances to-
539 ward explainable or interpretable artificial intelligence have recently
540 been made (86).

541 We believe that climate-network analyses and ANNs can gain-
542 fully combine (37, 87). The ANNs' strength of being able to learn
543 complex non-linear relationships in the presented data and the
544 climate networks' ability to identify and compress/merge spatially
545 dispersed information about cooperativity and their potential to pro-
546 vide a physical interpretation makes them well-fitting complements
547 for climate-phenomena forecasting.

548 Outlook

549 The above (incomplete) list of successful applications of network
550 theory to climate phenomena demonstrates the potential of this
551 approach. We argue that it complements established concepts and
552 schemes with a new possibility to reveal precursor processes or
553 even entire causal chains of climate phenomena. Network theory
554 applied to climate science is still in its infancy and the subject of
555 ongoing research. The analyses of complex climate phenomena
556 such as the ones discussed above require individual case-by-case
557 approaches and there are no simple general recipes yet. Climate
558 networks are versatile tools for exploratory analysis to uncover
559 spatial and temporal patterns in the data, which may potentially
560 lead with domain expertise to new forecasting methods.

561 The examples highlighted in this Perspective can, however,
562 serve as useful analogies/templates for a network-based forecast-
563 ing of climate phenomena that are similar to them. For instance,
564 the example of El Niño can serve as a template to forecast other
565 large-scale cooperative phenomena like the Indian Ocean Dipole
566 or the Atlantic El Niño. As in the case of the Amazon droughts, the
567 quantification of the impacts of SST patterns on rainfall anomalies
568 over adjacent continents should be possible also for other tropical
569 regions where land-ocean temperature gradients drive moisture
570 flow and hence rainfall anomalies. The approach developed for
571 the extreme rainfall prediction in the Central Andes should be
572 applicable also to other regions where interactions between sub-
573 tropical and extratropical weather phenomena are relevant, such

as in North America or eastern Asia. Developed for forecasting
the Indian summer monsoon, the tipping elements approach is
applicable to other climate and weather phenomena that exhibit
a critical transition. In particular, it could be applied to other mon-
soon systems in West and East Africa, and also North and South
America. Finally, the PCMC algorithm is particularly useful if the
primary goal of an analysis is an understanding of the underlying
mechanisms of a regarded phenomenon.

Network theory applied to climate science is rapidly developing,
but there are still open challenges in the realm of application, as
well as challenges of methodological nature:

Since climate networks are constructed from observational data
via similarity measures, e.g., correlations, their underlying physi-
cal processes may not be immediately apparent. Uncovering the
physical processes can lead to a better understanding of the re-
garded system, which could translate into better predictions within
the network framework or improved numerical models. Causally
interpretable networks and machine learning techniques could be
instrumental in uncovering the underlying processes. As recently
argued regarding the role of theory in modelling-dominated climate
science (88), a delicate balance between, and a skillful combina-
tion of, observations, theory and application-driven simulations (be
it through numerical modelling or network methods, or rather both)
may provide the best path forward.

Then, there are some challenges related to the data itself: First,
as an entirely data-dependent approach, network analysis may
be subject to the underlying uncertainty in the data. Based on
experience, the network-based schemes appear to be robust, see,
e.g., (32) and in practice data uncertainty might not be a significant
issue. However, this remains to be studied systematically.

Another question is, how to incorporate multi-variate data sets?
Most current approaches construct climate networks by relying on
a single physical quantity, e.g., temperature or precipitation data.
For instance, reanalysis data sets offer a wide range of physical
quantities at each grid point. Exploiting multi-variate networks,
also called multi-layer networks, can enable new ways for both un-
derstanding the underlying phenomena and also finding improved
prediction schemes.

New reanalysis data, e.g., ERA5 (89), which create ensembles
of plausible trajectories instead of only a single one, as previous
products mostly did, may improve predictions, e.g., when uncertain
input data can be identified and possibly omitted or down-weighted.
Also, robustness-tests for the prediction methods to intra-ensemble
uncertainties are now becoming feasible. Climate networks are
often constructed only based on one assimilation product, often
due to the lack of viable alternatives, and in the future, systematic
inter-data-set comparisons would be desirable.

Apart from these "data uncertainty problems", there is also
the case where there is not enough data available: for instance,
how can the often short observational records be dealt with? This
is especially relevant for extreme events, which are by definition
rare, and only a few extreme events might be on record to validate
more complex prediction models based on network characteris-
tics. Possible solutions could be applying the prediction methods
from network theory to the output of GCM runs or validating on
corresponding phenomena at different geographical locations. Ad-
ditionally, long paleoclimatological records, for instance, tree-ring
or coral-based reconstructions, could provide opportunities to val-
idate complex prediction models. Finally, when looking into the
future of the method itself: Does climate change impact a fore-
casting scheme and does it need to be extended accordingly, e.g.,

635 by evolving networks? Statistical prediction methods in general
636 entail stationarity assumptions, which may or may not be fulfilled
637 in a changing climate, where unprecedented configurations could
638 appear. Applying the prediction schemes to GCM future scenario
639 outputs or an understanding of a method's underlying processes
640 could reveal if and how schemes should be modified.

641 Most importantly, and in spite of all these standing challenges,
642 network analysis can serve both as a toolbox to develop early-
643 warning schemes as well as concrete leads or as a scientific in-
644 spiration for identifying physical mechanisms that relate spatially
645 and/or temporally distant observations, where no connection was
646 suspected before.

647 These first successes encourage us to invite the research com-
648 munity to intensively investigate the applicability of the network
649 approach to climate dynamics, but also to other data-rich problems
650 of non-local nature. We are confident that based on network ap-
651 proaches, critical advances are possible in the understanding and
652 prediction of emerging phenomena, with topics ranging from jet-
653 stream dynamics, sea-ice melting and earthquakes to epidemics
654 containment and physiological-systems collapse.

655 **Data Availability.** There are no data underlying this work.

656 Acknowledgments

657 We would like to thank the anonymous reviewers for their very
658 constructive comments and suggestions. J.L., J.F., E.S. acknowl-
659 edge the support of the EPICC project funded by the German
660 Federal Ministry for the Environment, Nature Conservation and Nu-
661 clear Safety (BMU) (18_II_149_Global_A_Risikovorhersage). N.B.
662 acknowledges funding by the Volkswagen foundation and the Euro-
663 pean Union's Horizon 2020 research and innovation program under
664 grant agreement No. 820970 (TiPES). C.C. acknowledges funding
665 by DFG/FAPESP (IRTG 1740/TRP 2015/50122-0). S.H. thanks
666 the Israel Science Foundation (Grant no. 189/19), the joint China-
667 Israel Science Foundation (Grant no. 3132/19), the BIU Center
668 for Research in Applied Cryptography and Cyber Security, NSF-
669 BSF Grant no. 2019740, the EU H2020 project RISE, and DTRA
670 Grant no. HDTRA-1-19-1-0016 for financial support. M.K. has re-
671 ceived funding from the European Union's Horizon 2020 research
672 and innovation programme under the Marie Skłodowska-Curie
673 grant agreement (No. 841902). J.K. acknowledges support from
674 the Russian Ministry of Science and Education Agreement (No.
675 13.1902.21.0026). V.S. acknowledges the support from the Rus-
676 sian Foundation for Basic Research (RFBR) (No. 20-07-01071).

677

678 1 S. Hallegate, A cost effective solution to reduce disaster losses in developing countries: Hydro-
679 meteorological services, early warning, and evacuation. Policy Research Working Paper 6058
680 (The World Bank, 2012).
681 2 L. M. Braman *et al.*, Climate forecasts in disaster management: Red Cross flood operations in
682 West Africa, 2008. *Disasters* **37**, 144-164 (2013).
683 3 E. Kintisch, How a 'Godzilla' El Niño shook up weather forecasts. *Science* **352**, 1501-1502
684 (2016).
685 4 A. S. T. de la Poterie *et al.*, Understanding the use of 2015–2016 El Niño forecasts in shaping
686 early humanitarian action in Eastern and Southern Africa. *Int. J. Disaster Risk Reduct.* **30**,
687 81-94 (2018).
688 5 S. M. Moore *et al.*, El Niño and the shifting geography of cholera in Africa. *Proc. Natl. Acad.*
689 *Sci. USA* **114**, 17, 4436-4441 (2017).
690 6 V. Petoukhov *et al.*, Role of quasiresonant planetary wave dynamics in recent boreal spring-to-
691 autumn extreme events. *Proc. Natl. Acad. Sci. USA* **113**, 25, 6862-6867 (2016).
692 7 N. Sandhu, J. Hussain, H. Matlay, Barriers to finance experienced by female owner/managers
693 of marginal farms in India. *Journal of Small Business and Enterprise Development* **19**, 4,
694 640–655 (2012).
695 8 P. Bauer, A. Thorpe, G. Brunet, The quiet revolution of numerical weather prediction. *Nature*,
696 **525**(7567), 47-55 (2015).

9 L. F. Richardson, Weather prediction by numerical process (Cambridge Univ. Press, Cam- 697
bridge, UK, 1922). 698
10 J. G. Charney, R. Fjorftoft, J. von Neumann, Numerical integration of the barotropic vorticity 699
Equation. *Tellus* **2**, 4, 237–254 (1950). 700
11 World Meteorological Organization. Seamless Prediction of the Earth System: From Minutes 701
to Months. WMO No. 1156 (World Meteorological Organization, Geneva, Switzerland, 2015). 702
12 R. B. Alley, K.A. Emanuel, F. Zhang, Advances in weather prediction. *Science*, **363**(6425), 703
342-344, (2019). 704
13 F. Zhang *et al.*, What is the predictability limit of midlatitude weather? *Journal of the Atmo-* 705
spheric Sciences, **76**(4), 1077-1091, (2019). 706
14 World Climate Research Programme, Near-Term Climate Prediction. 707
[https://www.wcrp-climate.org/component/content/article/695-gc-near-term-climate-](https://www.wcrp-climate.org/component/content/article/695-gc-near-term-climate-overview?catid=138&Itemid=538) 708
[overview?catid=138&Itemid=538](https://www.wcrp-climate.org/component/content/article/695-gc-near-term-climate-overview?catid=138&Itemid=538). Accessed 31 July 2020. 709
15 A. Mariotti, P. M. Ruti, M. Rixen, Progress in subseasonal to seasonal prediction through a 710
joint weather and climate community effort. *npj. Clim. Atmos. Sci.* **1**, 4 (2018). 711
16 F. Vitart, A. W. Robertson, The sub-seasonal to seasonal prediction project (S2S) and the 712
prediction of extreme events. *npj. Clim. Atmos. Sci.* **1**, 3 (2018). 713
17 F. Hourdin *et al.*, The art and science of climate model tuning. *Bulletin of the American Meteoro-* 714
logical Society, **98**(3), 589-602 (2017). 715
18 G. T. Walker, Correlations in seasonal variations of weather. I. A further study of world weather. 716
Mem. Indian Meteorol. Dep., **24**, 275-332 (1924). 717
19 M. Bennet *et al.*, Huygens's clocks. *Proc. of the Royal Society of London. Series A: Mathemat-* 718
ical, Physical and Engineering Sciences **458**, 2019, 563-579 (2020). 719
20 A. Pikovsky, M. Rosenblum, J. Kurths, Synchronization: A universal concept in nonlinear sci- 720
ences (Cambridge University Press, Cambridge, UK, 2003). 721
21 M. Newman, Networks: An introduction (Oxford University Press, Oxford, UK, 2010). 722
22 R. Cohen and S. Havlin, Complex Networks: Structure, Robustness and Function (Cambridge 723
University Press, Cambridge, UK, 2010) 724
23 A. L. Barabasi, Network Science (Cambridge University Press, Cambridge, UK, 2016). 725
24 J. Fan *et al.*, Statistical physics approaches to the complex Earth system. *Physics Reports* **896**, 726
1-84, (2021). 727
25 Y. Zou, R. V. Donner, N. Marwan, J. F. Donges, J. Kurths, Complex network approaches to 728
nonlinear time series analysis. *Physics Reports*, **787**, 1-97, (2019). 729
26 N. Molkenhuth, K. Rehfeld, N. Marwan, N., J. Kurths, Networks from flows-from dynamics to 730
topology. *Scientific reports*, **4**(1), 1-5 (2014). 731
27 E. N. Lorenz, Deterministic non-periodical flow. *J. Atmos. Sci.* **20**, 130–141 (1963). 732
28 E. A. Allen, E. Damaraju, T. Eichele, L. Wu, V. D. Calhoun, EEG signatures of dynamic func- 733
tional network connectivity states. *Brain topography*, **31**(1), 101-116 (2018). 734
29 A. A. Tsonis, P. J. Roebber, The architecture of the climate network. *Physica A* **333**, 497-504 735
(2004). 736
30 K. Yamasaki, A. Gozolchiani, S. Havlin, Climate networks around the globe are significantly 737
affected by El Niño. *Phys. Rev. Lett.* **100**, 228501(2008). 738
31 J. F. Donges, Y. Zou, N. Marwan, J. Kurths, Complex networks in climate dynamics. *The Euro-* 739
pean Physical Journal Special Topics, **174**(1), 157-179 (2009). 740
32 J. Ludescher *et al.*, Improved El Niño forecasting by cooperativity detection. *Proc. Natl. Acad.* 741
Sci. USA **110**, 11742-11745 (2013). 742
33 J. Ludescher *et al.*, Very early warning of next El Niño. *Proc. Natl. Acad. Sci. USA* **111**, 2064- 743
2066 (2014). 744
34 V. Rodríguez-Méndez, V. M. Eguíluz, E. Hernández-García, J. J. Ramasco, Percolation-based 745
precursors of transitions in extended systems. *Sci. Rep.* **6**, 29552 (2016). 746
35 Q. Y. Feng *et al.*, ClimateLearn: a machine-learning approach for climate prediction using 747
network measures. *Geosci. Model Dev. Discuss.* doi: 10.5194/gmd-2015-273 (2016). 748
36 J. Meng *et al.*, Forecasting the magnitude and onset of El Niño based on climate network. *New* 749
Journal of Physics **20**(4), 043036 (2018). 750
37 P. D. Nooteboom, Q. Y. Feng, C. López, E. Hernández-García, H. A. Dijkstra, Using network 751
theory and machine learning to predict El Niño. *Earth Syst. Dynam.* **9**, 969-983 (2018). 752
38 P. J. Petersik and H. A. Dijkstra, Probabilistic Forecasting of El Niño Using Neural Network 753
Models. *Geophys. Res. Lett.* **47**, 6, e2019GL086423 (2020). 754
39 C. Ciemer *et al.*, An early-warning indicator for Amazon droughts exclusively based on 755
tropical Atlantic sea surface temperatures. *Environmental Research Letters* **15**, 9, 094087, 756
<https://doi.org/10.1088/1748-9326/ab9c9f> (2020). 757
40 N. Boers *et al.*, Complex networks identify spatial patterns of extreme rainfall events of the 758
South American Monsoon System. *Geophys. Res. Lett.* **40**, 16, 4386-4392 (2013). 759
41 N. Boers *et al.*, Prediction of extreme floods in the eastern Central Andes based on a complex 760
networks approach. *Nature Commun.* **5**, 5199 doi: 10.1038/ncomms6199 (2014). 761
42 N. Malik, B. Bookhagen, N. Marwan, J. Kurths, Analysis of spatial and temporal extreme mon- 762
soonal rainfall over South Asia using complex networks. *Clim. Dyn.* **39**, 971-987 (2012). 763
43 V. Stolbova, P. Martin, B. Bookhagen, N. Marwan, J. Kurths, Topology and seasonal evolution 764
of the network of extreme precipitation over the Indian subcontinent and Sri Lanka. *Nonlin.* 765
Processes Geophys. **21**, 901–917 (2014). 766
44 V. Stolbova, E. Surovyatkina, B. Bookhagen, J. Kurths, Tipping elements of the Indian mon- 767
soon: Prediction of onset and withdrawal. *Geophys. Res. Lett.* **43**, 8, 3982-3990 (2016). 768
45 M. Kretschmer, D. Coumou, J. F. Donges, J. Runge, Using causal effect networks to analyze 769
different arctic drivers of midlatitude winter circulation. *J. Clim.* **29**, 4069-4081 (2016). 770
46 M. Kretschmer, J. Runge, D. Coumou, Early prediction of extreme stratospheric polar vortex 771
states based on causal precursors. *Geophys. Res. Lett.* **44**, 16, 8592-8600 (2017). 772
47 D. S. Pai, R. M. Nair, Summer monsoon onset over Kerala: new definition and prediction. *J.* 773
Earth Syst. Sci. **118**, 123-135 (2009). 774
48 D. I. Domeisen *et al.*, The role of the stratosphere in subseasonal to seasonal prediction Part I: 775
Predictability of the stratosphere. *J. Geophys. Res. Atmos.*, **125**, e2019JD030920 (2020). 776
49 E. S. Sarachik, M. A. Cane, *The El Niño-Southern Oscillation phenomenon* (Cambridge Uni- 777
versity Press, Cambridge, UK, 2010). 778
50 A. Timmermann *et al.*, El Niño-Southern Oscillation complexity. *Nature* **559**, 535-545 (2018). 779
51 M. J. McPhaden, A. Santoso, W. Cai (Eds.), *El Niño Southern Oscillation in a Changing Cli-* 780

781 *mate.* (John Wiley & Sons, Hoboken, NJ, USA, 2020).

782 52 A. G. Barnston *et al.*, Skill of real-time seasonal ENSO model predictions during 2002–11:
783 Is our capability increasing?. *Bulletin of the American Meteorological Society*, **93**(5), 631–651
784 (2012).

785 53 M. J. McPhaden, Playing hide and seek with El Niño, *Nature Climate Change*, **5**(9), 791–795,
786 doi:10.1038/nclimate2775 (2015).

787 54 International Research Institute for Climate and Society. [https://iri.columbia.edu/our-](https://iri.columbia.edu/our-expertise/climate/forecasts/enso/2013-December-quick-look/?enso_tab=enso-iri_plume)
788 [expertise/climate/forecasts/enso/2013-December-quick-look/?enso_tab=enso-iri_plume.](https://iri.columbia.edu/our-expertise/climate/forecasts/enso/2013-December-quick-look/?enso_tab=enso-iri_plume)
789 Accessed February 12 2021.

790 55 A. Gozolchiani, K. Yamasaki, S. Havlin, The Emergence of El-Niño as an Autonomous Com-
791 ponent in the Climate Network. *Phys. Rev. Lett.* **107**, 148501 (2011).

792 56 E. Kalnay *et al.*, The NCEP/NCAR 40-year reanalysis project. *Bull. Am. Meteorol. Soc.* **77**(3),
793 437–471 (1996).

794 57 B.P. Kirtman, The COLA anomaly coupled model: Ensemble ENSO prediction. *Mon. Weather*
795 *Rev.* **131**, 2324–2341 (2003).

796 58 D. Chen, M.A. Cane, El Niño prediction and predictability. *J. Comput. Phys.* **227**, 3625–3640
797 (2008).

798 59 M. A. De Castro Santos, D. A. Vega-Oliveros, L. Zhao, L. Berton, Classifying El Niño-Southern
799 Oscillation Combining Network Science and Machine Learning. *IEEE Access* **8**, 55711–55723
800 (2020).

801 60 S. L. Lewis, P. M. Brando, O. L. Phillips, G. M. van der Heijden, D. Nepstad, The 2010 Amazon
802 drought. *Science*, **331**(6017), 554–554 (2011).

803 61 T. E. Lovejoy and C. Nobre, Amazon tipping point: Last chance for action. *Sci. Adv.* **5**:eaba2949
804 (2019).

805 62 R. Brienen *et al.*, Long-term decline of the Amazon carbon sink. *Nature* **519**, 344–348 (2015).

806 63 C. Vera, G. Silvestri, B. Liebmann, P. González, Climate change scenarios for seasonal precip-
807 itation in South America from IPCC-AR4 models. *Geophys. Res. Lett.* **33**, 13, L13707 (2006).

808 64 J. A. Marengo, J. C. Espinoza, Extreme seasonal droughts and floods in Amazonia: causes,
809 trends and impacts. *International Journal of Climatology*, **36**, 3, 1033–1050 (2016).

810 65 N. Boers *et al.*, Complex networks reveal global pattern of extreme-rainfall teleconnections.
811 *Nature* **566**, 373–377 (2019).

812 66 E. D. Surovyatkina, Y. A. Kravtsov, J. Kurths, Fluctuation growth and saturation in nonlinear
813 oscillator on the threshold of bifurcation of spontaneous symmetry breaking. *Phys. Rev. E* **72**,
814 4, 046125 (2005).

815 67 CPC Global Unified Gauge-Based Analysis of Daily Precipitation, NOAA Physical Sciences
816 Laboratory. <https://psl.noaa.gov/data/gridded/data.cpc.globalprecip.html>. Accessed June 8
817 2021.

818 68 Potsdam Institute for Climate Impact Research, Monsoon Page. [https://www.pik-](https://www.pik-potsdam.de/services/infodesk/forecasting-indian-monsoon)
819 [potsdam.de/services/infodesk/forecasting-indian-monsoon](https://www.pik-potsdam.de/services/infodesk/forecasting-indian-monsoon). Accessed July 31 2020.

820 69 M. P. Baldwin, T. J. Dunkerton, Stratospheric harbingers of anomalous weather regimes. *Sci-*
821 *ence* **294**, 581–584 (2001).

822 70 L. Jia *et al.*, Seasonal prediction skill of northern extratropical surface temperature driven by
823 the stratosphere. *J. Clim.* **30**, 4463–4475 (2017).

824 71 J. Runge *et al.*, Detecting and quantifying causal associations in large nonlinear time series
825 datasets. *Sci. Adv.* **5**, eaa4996 doi: 10.1126/sciadv.aau4996 (2019).

826 72 J. Runge *et al.*, Inferring Causation from Time Series in Earth System Sciences. *Nature Com-*
827 *mun.* **10**, 2553 (2019).

828 73 European Centre for Medium-Range Weather Forecasts, ERA-40. Data are available at
829 <http://apps.ecmwf.int/datasets/data/era40-daily/levtype=pl/>. Accessed July 31 2020.

830 74 National Center for Environmental Prediction/National Center for Atmospheric Research, Re-
831 analysis 1. Data available at <https://psl.noaa.gov/data/gridded/data.ncep.reanalysis.html>. Ac-
832 cessed July 31 2020.

833 75 G. Di Capua *et al.*, Long-Lead Statistical Forecasts of the Indian Summer Monsoon Rainfall
834 Based on Causal Precursors. *Weather and Forecasting* **34**, 5, 1377–1394 (2019).

835 76 P. Pfeleiderer, C. Schleussner, T. Geiger, M. Kretschmer, Robust Predictors for Seasonal Atlantic
836 Hurricane Activity Identified with Causal Effect Networks. *Weather and Climate Dynamics* **1**,
837 313–324 (2020).

838 77 D. Maraun *et al.*, Towards Process-Informed Bias Correction of Climate Change Simulations.
839 *Nature Climate Change* **7**, 11, 764–773 (2017).

840 78 M. Dobrynin *et al.*, Improved teleconnection-based dynamical seasonal predictions of boreal
841 winter. *Geophys. Res. Lett.* **45**, 8, 3605–3614 (2018).

842 79 P. Nowack, J. Runge, V. Eyring, J. D. Haigh, Causal networks for climate model evaluation and
843 constrained projections. *Nature communications*, **11**(1), 1–11 (2020).

844 80 I. Goodfellow, Y. Bengio, A. Courville, *Deep learning* (MIT press, Massachusetts, USA, 2016).

845 81 M. Reichstein *et al.*, Deep learning and process understanding for data-driven Earth system
846 science. *Nature* **566**, 195–204 (2019).

847 82 Y. G. Ham, J. H. Kim, J. J. Luo, Deep learning for multi-year ENSO forecasts. *Nature* **573**,
848 568–572 (2019).

849 83 M. Saha, P. Mitra, R. S. Nanjundiah, Deep learning for predicting the monsoon over the homo-
850 geneous regions of India. *J. Earth Syst. Sci.* **126**, 54 (2017).

851 84 D. Rolnick *et al.*, Tackling climate change with machine learning. arXiv:1906.05433 (2019).

852 85 A. McGovern *et al.*, Making the Black Box More Transparent: Understanding the Physical
853 Implications of Machine Learning. *Bull. Amer. Meteor. Soc.* **100**, 2175–2199 (2019).

854 86 W. Samek, K. R. Müller, “Towards Explainable Artificial Intelligence” in *Explainable AI: Inter-*
855 *preting, Explaining and Visualizing Deep Learning*, W. Samek, G. Montavon, A. Vedaldi, L.
856 Hansen, K. R. Müller (Eds.). https://doi.org/10.1007/978-3-030-28954-6_1 (Springer Nature,
857 Cham, Switzerland, 2019).

858 87 H. A. Dijkstra, P. Petersik, E. Hernández-García, C. López, The application of machine learning
859 techniques to improve El Niño prediction skill. *Front. Phys.* **7**, 153 (2019).

860 88 K. Emanuel, The Relevance of Theory for Contemporary Research in Atmospheres, Oceans,
861 and Climate. *AGU Advances*, **1**, e2019AV000129 (2020).

862 89 European Centre for Medium-Range Weather Forecasts, ERA5.
863 <https://www.ecmwf.int/en/forecasts/datasets/reanalysis-datasets/era5>. Accessed February 12
864 2021.